Al-Azhar University Civil Engineering Research Magazine (CERM)
Vol. (41) No. (1) January, 2019

Monitoring Crack Propagation in Reinforced Concrete Coupled Shear Wall Supported on Two Columns

1- Eng. Amir Abd Elfadeel Esmaeil Ghanem,
2- - Dr. Nasser Fekry Hasan, 3- Dr. Heba M. Issa

1- Teaching Assistant at Misr High Institute for engineering and technology in Mansoura
2- Associate Professor Structural Engineering Department, Faculty of Engineering, Cairo University
3- Assistant Professor of Reinforced Concrete Structures, Housing and Building National Research Institute.

ملخص البحث :

الهدف من هذه الدراسة هو دراسة تأثير انتشار الشروخ في حدود اللدن و ما بعد اللدن. ولهذا تم عمل دراسة لحالات ببرنامج تحليلي يستخدم طريقة العناصر المحدودة لعدد ثمانية عشر حالة مع الاخذ في الاعتبار الشروخ و انهيار الخرسانة في الضغط و الخضوع في حديد التسليح و ذلك تحت تأثير متغيرات و هي الاجهاد الأقصى للخرسانة و نسبة الصلابة بين الاعمدة و حوائط القص و نسبة التسليح في كل من في العناصر الانشائية و ذلك علي كل من الحمل الاقصى الافقي و الممطولية. و أظهرت النتائج أن تأثير نسبة الصلابة بين الاعمدة و حوائط القص علي انتشار الشروخ الاولية و شروخ القص أكبر خاصا علي الكمرة الانتقالية.

Abstract:

Many efforts have been made to monitor the cracking behavior in RC structures in the last two decades. The objective of this paper is to present the results of a theoretical study aimed at monitoring the behavior of coupled shear wall system in elastic and post elastic stage, also drift at each story, stress and strain for both concrete and reinforcement, and cracks propagation. Therefore, a case study was assumed, where three-dimensional, non-linear finite element analysis was carried out for eighteen samples taking into consideration cracking; crushing of concrete, and yielding of rebar.

The results were reported as the effect of characteristic strength; stiffness ratio between columns and walls, on the ultimate horizontal load capacity; the ductility of the entire system. The results demonstrate that stiffness ratio between shear walls and supported columns is more crucial on the response of the coupled system rather than characteristic strength, and the position of first flexural and shear cracks are predominated by transfer beam.

Keywords: Coupled shear walls supported on columns; Earthquake; Non-linear finite configuration, Cracks in shear walls.

1. Introduction:

Morgan [4] studied seven stories coupled shear walls supported on columns under vertical loads only. This study included material linearity and non-linearity of two dimensional reinforced concrete structures under the action of monotonically increased loads. This study based on finite element analysis by using of (NARCS10) program. The finite element analysis by (NARCS10) program included iso-parametric quadrilateral element, and steel reinforcement was modeled using two nodes discrete bar element as well as smeared steel element. It concludes that transfer beam must have a height not less than 20% of the clear span of the lower wide floor, increasing or decreasing the amount of main steel of this type of structures has inconsequential effect on the ultimate load of the wall. This means that, the failure of the wall is mainly controlled by the ultimate compressive strength of concrete, and the use of 4, 5 and 6 nodes quadrilateral elements gives reasonable accuracy for the results.

Khaled [5] studied the same system of Morgan [4] using a finite element program (ANSYS). In addition to pushover analysis, and addressing the effect of stiffness variation of columns, coupling beams, transfer beams and link beams. Moreover, scrutinized the load path dependence for gravitational and pushover combinations. It concludes that the stress concentration pattern significantly differs depending on the type of loading. Geometric discontinuity regions capture the highest damage evolution rate. For example, under gravitational loading stress concentration takes place at the column-wall junction and also in the transfer and the link beams. On the other hand, for lateral loading the highest tensile stresses occur at the column-wall junction of the loaded side and in coupling beams. Redistribution of stresses is evident through the course of loading with emphasis to the relative column to coupled shear wall stiffness. In turn, the position of the maximum bending stresses shifts from the base upwards with the progress of loading. The same system of Khaled [5], as an example, used to validate the use of "ANSYS (14)" [1] program, and the results obtained from the analysis are nearly the same results of Khaled [5].

The main objectives of present work are to provide the several parameters required to have a better understanding of the behavior of the coupled shear walls supported on columns under quasi-static loading. The main objectives can be summarizing as the following:

1- Understanding the behavior of the coupled system taking into consideration the effect of material nonlinearity in vertical loading besides static pushover analysis.

2- Analyzing the response of the coupled system on the ultimate horizontal load capacity and the ductility of all main members under the effect of characteristic strength, stiffness ratio between columns and walls, and reinforcement ratio

2. Case Study

2.1 Main Parameters

The main parameters taken into consideration are listed below in Table (1):

Sample number	Main parameters					
	(1) f'_c (MPa)	(2) Reinforcement ratio (μ%)				(3) $\left[\frac{t\_column}{t\_wall}\right]$ %
		column	Transfer beam	wall	Connecting beam	
1	35	0.76%	0.68%	0.62%	0.92%	37.5%
2	35	0.76%	6.5%	0.62%	0.92%	37.5%
3	35	3.7%	6.5%	1.17%	3.9%	37.5%
4	35	0.76%	0.68%	0.62%	0.92%	51.25%
5	35	0.76%	6.5%	0.62%	0.92%	51.25%
6	35	3.7%	6.5%	1.17%	3.9%	51.25%
7	45	0.76%	0.68%	0.62%	0.92%	37.5%
8	45	0.76%	6.5%	0.62%	0.92%	37.5%
9	45	3.7%	6.5%	1.17%	3.9%	37.5%
10	45	0.76%	0.68%	0.62%	0.92%	51.25%
11	45	0.76%	6.5%	0.62%	0.92%	51.25%
12	45	3.7%	6.5%	1.17%	3.9%	51.25%
13	60	0.76%	0.68%	0.62%	0.92%	37.5%
14	60	0.76%	6.5%	0.62%	0.92%	37.5%
15	60	3.7%	6.5%	1.17%	3.9%	37.5%
16	60	0.76%	0.68%	0.62%	0.92%	51.25%
17	60	0.76%	6.5%	0.62%	0.92%	51.25%
18	60	3.7%	6.5%	1.17%	3.9%	51.25%

2.2 Geometry Dimensions

Plan area (20×30 m), Shear wall cross-section (0.5×4 m), Columns cross-section(0.5×1.5 m), Connecting beams cross-section(0.5×0.6 m), Transfer beam cross-section(0.5×1.5 m). The plane and elevation of the case study are shown in Figure (1).

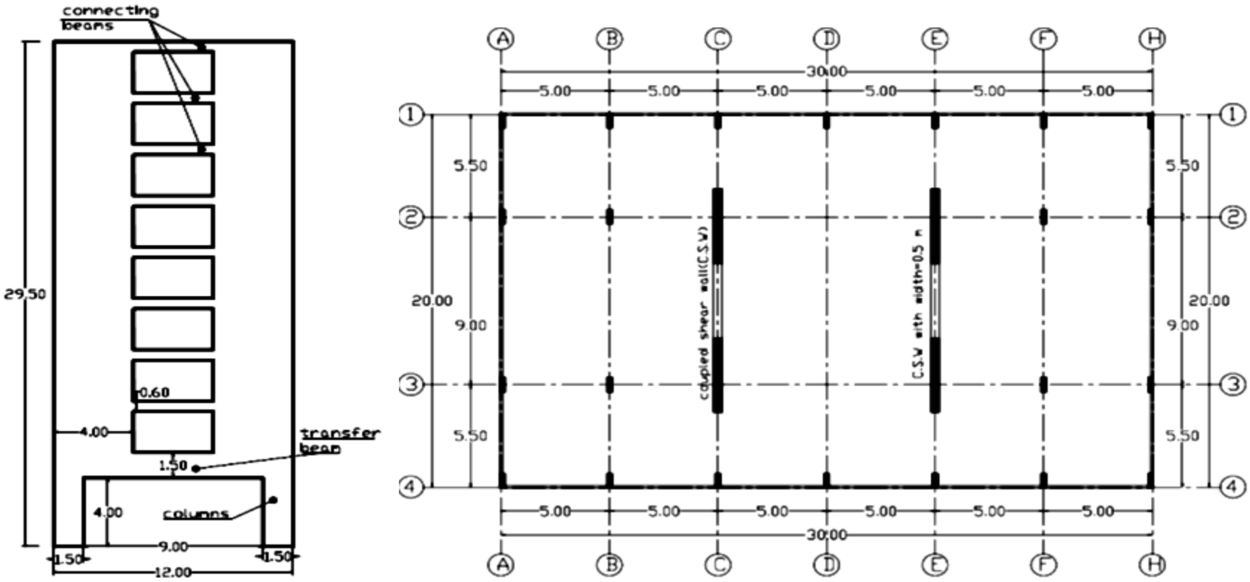

Figure 1: Elevation and plan of the coupled shear walls supported on columns

2.3 Reinforcement Ratio

There are three collections of steel reinforcement for entire structural elements as shown in Table (2). Collection one of reinforcement contains the ratios 0.76%,0.68%,0.62% and 0.92% for columns, transfer beam, walls and connecting beams respectively. Collection two of reinforcement includes the same ratios of collection one except for the transfer beam it is increased to 6.5%. Collection three of reinforcement includes the ratios 3.7%, 6.5%, 1.17% and 3.9% for columns, transfer beam, walls and connecting beams respectively. No additional moments occurred about the cross sections of the columns due to buckling.

Table 2: Details of reinforcement for collections (1, 2 and 3)

collection (1)	collection (2)	collection (3)
9ø25, 5ø16/M, 5ø14/M, 9ø25, 500, 4000, SEC(1-1), reinforcement ratio=0.62%	9ø25, 5ø16/M, 5ø14/M, 9ø25, 500, 4000, SEC(1-1), reinforcement ratio=0.62%	20ø25, 5ø16/M, 5ø14/M, 20ø25, 500, 4000, SEC(1-1), reinforcement ratio=1.17%
5ø25, 7ø10 /M stirrups, 1500, 5ø25, 500, SEC(2-2), reinforcement ratio=0.68%	40ø28, 7ø10 /M stirrups, 1500, 40ø28, 500, SEC(2-2), reinforcement ratio=6.5%	40ø28, 7ø10 /M stirrups, 1500, 40ø28, 500, SEC(2-2), reinforcement ratio=6.5%
9ø25, 5ø16/M, 7ø10/M stirrups, 500, 1.5, SEC(3-3), reinforcement ratio=0.8%	9ø25, 5ø16/M, 7ø10 /M stirrups, 500, 1.5, SEC(3-3), reinforcement ratio=0.8%	20ø25, 5ø16/M, 7ø10/M stirrups, 500, 1500, SEC(3-3), reinforcement ratio=3.7%
5ø18, 5ø8 /M stirrups, 600, 5ø18, 500, SEC(4-4), reinforcement ratio=0.92%	5ø18, 5ø8 /M stirrups, 600, 5ø18, 500, SEC(4-4), reinforcement ratio=0.92%	12ø25, 5ø8 /M stirrups, 600, 12ø25, 500, SEC(4-4), reinforcement ratio=3.9%

2.4 Vertical and Horizontal Loads

Factored vertical loads are calculated due to the weight of walls, coupling beams, columns, in addition to loads from the weight of slabs, where: live load=4 kN/m^2, flooring load =1.5 kN/m^2, weight of brick walls=1.5 kN/m^2, thickness of slabs= 220 mm. And distributed vertical loads/story =100 kN/m. Horizontal loads are calculated by the simplified response spectrum analysis using "ECP-203" [2] which horizontal loads are rectangular distribution with maximum load equals 500 kN at the top.

2.5 Definition of ductility

The ductility definition is the capability of the material/member to endure deformation beyond the elastic limit. The deformation utilized to evaluate the ductility may be strain, curvature, displacement or rotation. According to "H. J. Pam, A. K. H. Kwan and M. S. Islam" [6] it is better to express the ductility in terms of a dimensionless ductility factor (μ):

$$\mu = \left[\frac{\Delta max}{\Delta y}\right] \quad (1)$$

Where: (Δ_{max}) is the maximum deformation, when the crushing of concrete for any structural member occurs. And (Δ_y) is the yielding deformation, when the reinforcement for any structural element yields.

3. Finite Element Modeling

The finite element method using "ANSYS (14)" [1] package can be used to closely forecast the behavior of the coupled system which subjected to in-plane forces. The load-deflection behavior, crack propagation, first crack load, failure load, and failure mode can be predicted using the finite element method with an accuracy that is acceptable for engineering purposes. Furthermore, the program accounts for: (1) material non-linearity of both concrete and steel, (2) biaxial failure surface of concrete, (3) nonlinear stress-strain curve of steel and (4) concrete cracking and crushing.

3.1 Material properties

3.1.1 Concrete

Concrete in compression: the idealized stress strain curve as in ECP-03 [2] can be used for representing the actual behavior of concrete in compression. It consists of a parabola up to a strain of 0.002 and straight horizontal line up to a strain of 0.003.

Concrete in Tension: the tensile strength of concrete is very low and it might be generally about 10% of its compressive strength for normal concrete, but the tensile strength of high strength concrete can be calculated from equation (1) according to "Martinez, S., NiIson, AH., and Slate, F.O.,"[7]. In this study, concrete is assumed to behave as a linear elastic-brittle material in tension, and this is an essential factor causing the nonlinear behavior. Cracks are assumed to form in planes perpendicular to the direction of maximum principal tensile stress as soon as this reaches the specified concrete tensile strength.

$$f'_{sp} = 0.59\sqrt{f'_c} \text{ MPa} \quad (2)$$

The "SOLID65" element: A concrete 3D- solid element was use to model the behavior of concrete with reinforcing bars which requires linear isotropic and multi-linear isotropic material properties to properly model for concrete. The multi-linear isotropic material uses the Von-Misses failure criterion along with the "Willam and

Warnke," [8] model to define the failure of the concrete. "EX" is the initial tangent modulus of elasticity of the concrete (E_c) and "PRXY" is the Poisson's ratio (ν). The young's modulus for normal concrete (concrete with compressive strength less than (41 MPa) approximately) is depended on the following equation (2), and the young's modulus for high strength concrete (concrete with compressive strength in excess (41 MPa) approximately) is depended on the following equation (3) defined by "Martinez, S., NiIson, Ah., and Slate, F.O.," [7] .

$$E_c = 4700\sqrt{f_c'} \quad (MPa) \tag{3}$$

$$E_c = 3320\sqrt{f_c'} + 6900 \quad (MPa) \qquad (for\ 21\ MPa < f_c' < 83\ MPa) \tag{4}$$

Where a value of, f_c' equal to a cylinder compressive strength in (MPa) units, and Poisson's ratio is assumed to be 0.2 for concrete. The uniaxial compressive stress-strain relationship for the concrete model is obtained using the following equations (4, 5, 6) to calculate the multi-linear isotropic stress-strain curve for the concrete in compression "ACI code, MacGregor," [9] and this equation will be used in the present study:

$$f = \frac{E_c \varepsilon_c}{1+\left(\frac{\varepsilon_c}{\varepsilon_o}\right)^2} \tag{5}$$

$$\varepsilon_o = \frac{2f_c'}{E_c} \tag{6}$$

Where f is the stress at any strain ε_c and ε_o is the strain at the cylinder compressive strength f_c'. the multi-linear isotropic stress-strain curve, demands the first point of the curve to be entered by the user. It must satisfy Hooke's Law. The multi-linear curve is used to help for the convergence of the nonlinear solution algorithm.

The model that capable of predicting failure of concrete material is shown in Figure (2). Both cracking and crushing failure modes are taken into consideration. The two input strength parameters i.e., ultimate tensile and compressive strengths are demanded to define a failure surface of the concrete. Consequently, a criterion for failure of the concrete due multi-axial stress state can be calculated "Willam and Warnke" [8].

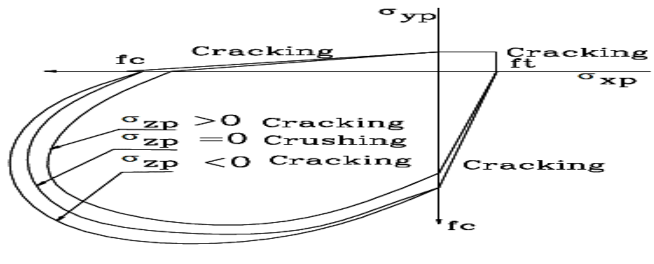

Figure 2: Failure surface of the concrete.

In concrete element, cracking occurs when the principal tensile stress in any directions lies outside the failure surface. After cracking, the young's modulus of concrete element is set to zero in the direction parallel to the principal tensile stress direction. Crushing takes place when all principal stresses are compressive and lie outside the failure surface. Thereafter, the young's modulus is set to zero in all directions, and the element effectively disappears.

For the implementation of the “Willam and Warnke” [8], material model in “ANSYS (14)” [1] requires defining nine constants as shown in Table (3).

3.1.2 Steel reinforcement

The “Link 8-3D” element is used to model steel reinforcement. This element is a uniaxial tension-compression element. The mechanical properties of steel are well-known and understood. Steel is homogeneous and has usually the same yield strength in tension and compression. In the present study reinforcing steel is modeled as a bilinear elasto-plastic material using the idealized stress-strain curve.

3.2 Material Modeling

Table 3: Material models for “SOLID65, LINK8 element”.

Material Model No.	Element Type	Material Properties	
1	SOLID65	**Linear Isotropic**	
		Elasticity Modulus, EX, is equal to $(\frac{f_1}{\varepsilon_1})$ at point (1) at the curve.	
		Poisson’s Ratio, PRXY, is equal to 0.20	
		Multi-linear Isotropic	
		Five coordinates are needed to represent the stress-strain curve for concrete, Figure (9).	
		Concrete	
		Open Shear Transfer Coeff.	0.2
		Closed Shear Transfer Coeff.	0.9
		Uniaxial Cracking Stress (Modules of rupture)	The concrete tensile strength f_t is typically 8% - 15% of the compressive strength and taken equal to 10% for normal concrete, and according to equation (1).
		Uniaxial Crushing Stress	The crushing stress value is taken from the stress-strain curve.
		Biaxial Crushing Stress	0
		Hydrostatic Pressure	0
		Hydro Biaxial Crush Stress	0
		Hydro Uniaxial Crush Stress	0
		Tensile Crack Factor	0
2	LINK8	**Linear Isotropic**	
		Elasticity Models, EX, is equal to 2×10^5MPa	
		Poisson’s Ratio PRXY, is equal to 0.30	
		Bilinear Isotropic	
		Yield Stresses follow the design material properties used for the experimental investigation.	
		Tangent Modulus is taken equal to Yield Stress.	

3.3 Modeling of coupled shear walls supported on columns by ANSYS program

Modeling of the coupled shear walls system is carried out where the node points of the solid elements coincide with the actual reinforcement locations as shown in Figure (3).

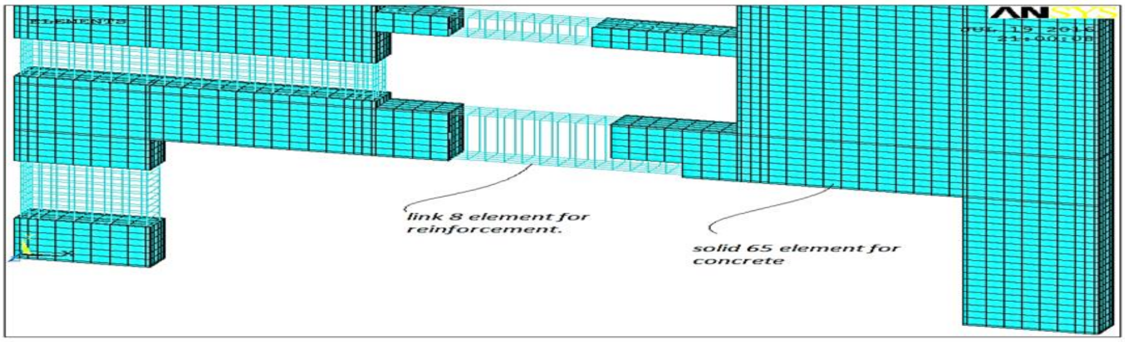

Figure 3: Modeling of the coupled shear walls system using ANSYS

4. Pushover Analysis and Results

Lateral loads represent one of the major concerns in high-rise buildings. Figure (7) shows the variation of top drift for all samples at different increments of loading. Apparently, the trend is nearly linear along the height at low load levels. However, at higher load increments, the drift at higher stories considerably differs and the trend tends to be non-linear. To illustrate the steps of loading as well as understanding the behavior of the coupled system, sample (12) can be taken as an example. At the beginning of loading, the structure is deformed until first flexure cracks have occurred at load 137.5 kN, therefore this load is considered as the first crack load (Pcr). At load 237.5 kN, first shear cracks are occurred, as well as increasing of flexure cracks propagation. By increasing the loading rate until load 575 kN that is considered yielding load (p_y), because of the beginning of yielding for stirrups of transfer beam, at this load, the value of drift at the top point is equal to 57.99 mm (Δ_y), as well as forming of the first plastic hinge at connecting beam no.4 from top as shown in Figure (5-a)- According to "Coull, A." [11], it is assumed that the plastic hinge forms at the middle third of the height of the coupled system. As a result of the beginning of yielding for stirrups of transfer beam, the elastic range would be considered ended and the post-elastic range would begin.

By helping the vector mode option of "ANSYS (14)" [1], it is observed that the regions of stress concentrations for the three principles stress at failure load as shown in figure (4). The first principle stress represents a maximum value (tension zone), and the third principle stress represents a minimum value (crushing zones). It is also found that further increasing of the loading rate would lead to the second plastic hinge at load 650 kN that is considered the failure load (P_u) because of the crushing of concrete for the supporting columns, Figure(5-b). At this load, it is also observed crushing of concrete for transfer beam and at the junction between connecting beams and the shear walls. In addition, the maximum drift (Δ_{max}) is founded equal to 71.46 mm as shown in Figure (6) the crack load failure for sample (12).

The main results for all samples are summarized in two main groups as shown in Tables (4) and (5): Group one includes samples number (1, 2, 3, 7, 8, 9, 13, 14, and 15) with stiffness ratio 37.5% between columns and walls. Group two includes samples number (4, 5, 6, 10, 11, 12, 16, 17, and 18) with stiffness ratio 51.25%.

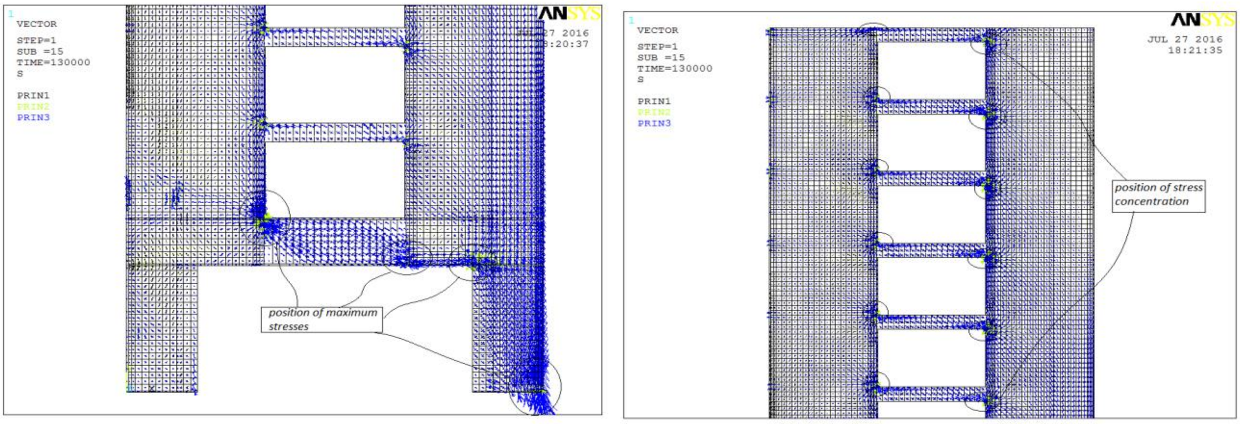

Figure 4: Principles stresses at failure load for sample (12)

Figure 5-a: 1st plastic hinge for sample (12) Figure 5-b: 2nd plastic hinge for sample (12)

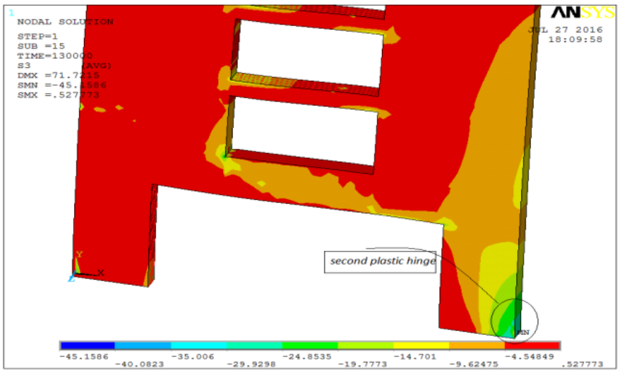

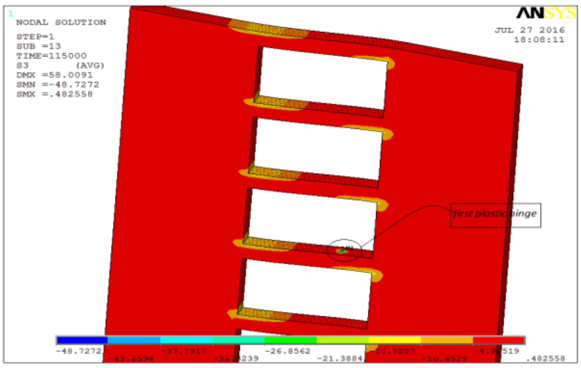

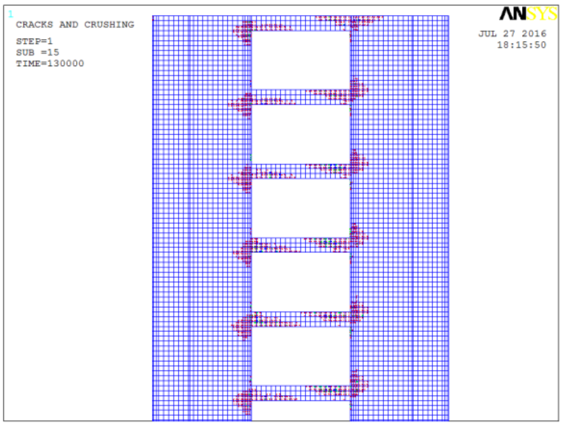

Figure 6: cracks pattern at failure load for sample (12).

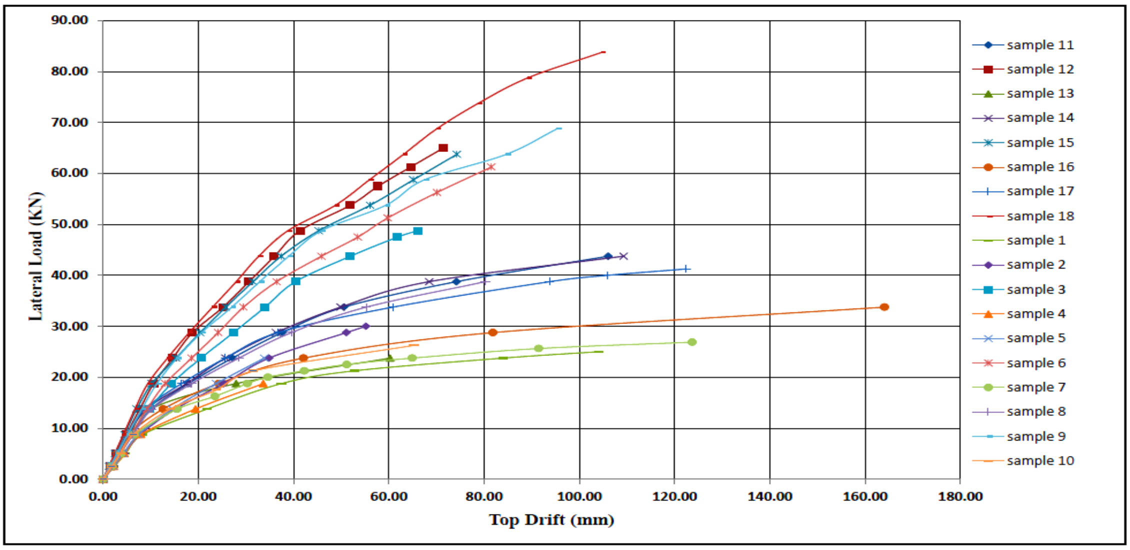

Figure 7: The variation of top drift for all samples at different increments of loading

Table (4) Results of Group one

	sample number	Pcr (ton)	Pv (ton)	Py (ton)	Pu (ton)	Yielding drift (mm)	Maxim. Drift (mm)	Fcu (mpa)	ductility ratio (%)
group one	1	8.75	13.75	13.75	25	21.93	104.22	35	4.75
	2	8.75	13.75	23.75	30	35.09	55.45	35	1.58
	3	13.75	18.75	38.75	48.75	40.59	66.26	35	1.63
	7	8.75	13.75	13.75	26.88	15.69	124.03	45	7.91
	8	8.75	18.75	23.75	38.75	28.68	80.49	45	2.81
	9	13.75	23.75	33.75	58.75	27.16	67.67	45	2.49
	13	8.75	13.75	18.75	23.75	28.04	60.37	60	2.15
	14	8.75	18.75	28.75	43.75	36.49	109.5	60	3.00
	15	13.75	23.75	33.75	63.75	25.89	74.28	60	2.87

Table (5) Results of Group two

	sample number	Pcr (ton)	Pv (ton)	Py (ton)	Pu (ton)	Yielding drift (mm)	Maxim. Drift (mm)	Fcu (mpa)	ductility ratio (%)
group two	4	8.75	13.75	13.75	18.75	19.52	33.64	35	1.72
	5	8.75	13.75	23.75	23.75	34.81	34.81	35	1.00
	6	13.75	23.75	51.25	61.25	60.02	81.51	35	1.36
	10	8.75	13.75	13.75	26.25	14.22	65.28	45	4.59
	11	8.75	18.75	23.75	43.75	27.33	106.05	45	3.88
	12	13.75	23.75	57.5	65	57.99	71.46	45	1.23
	16	8.75	13.75	18.75	33.75	24.31	164.06	60	6.75
	17	8.75	18.75	28.75	41.25	36.84	122.45	60	3.32
	18	13.75	23.75	73.75	83.75	78.99	104.66	60	1.32

Effect of characteristic strength (fcu) on ultimate horizontal load capacity, load of first shear cracks, load of first flexural cracks, and ductility can be illustrated by Figures 8, 9, 10, and 11 respectively. Samples are assembled through a table beneath every single bar-chart according to Table (6).

Table (6) Samples assembly for the case of effect (f_{cu})

	a	b	c	d	e	f
fcu=30	1	2	3	4	5	6
fcu=45	7	8	9	10	11	12
fcu=60	13	14	15	16	17	18

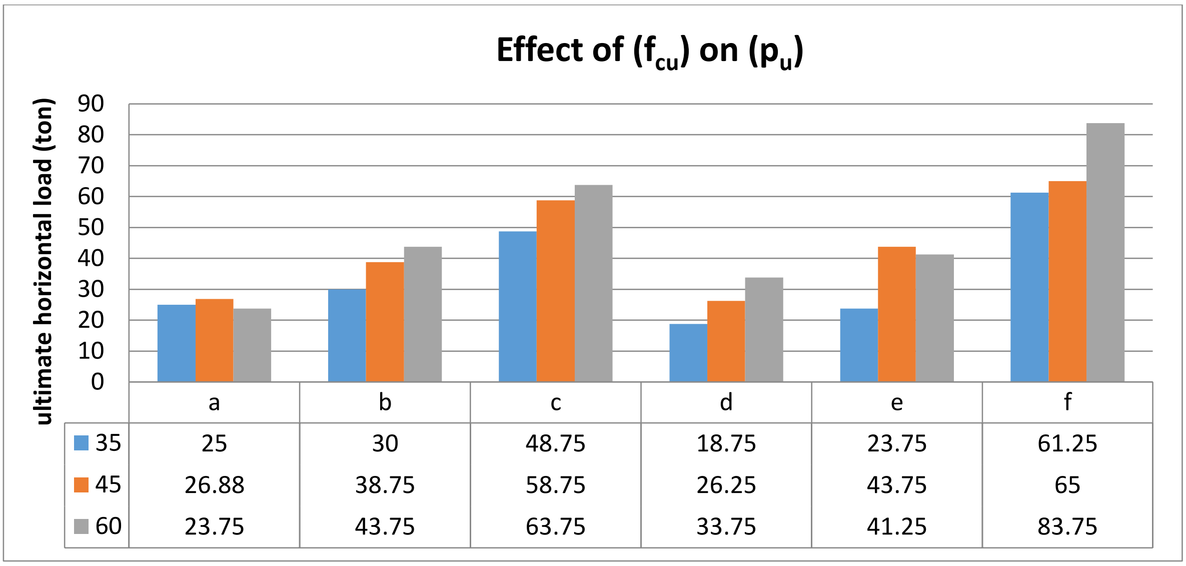

Figure 8: Effect of characteristic strength (f_{cu}) on ultimate horizontal load (p_u)

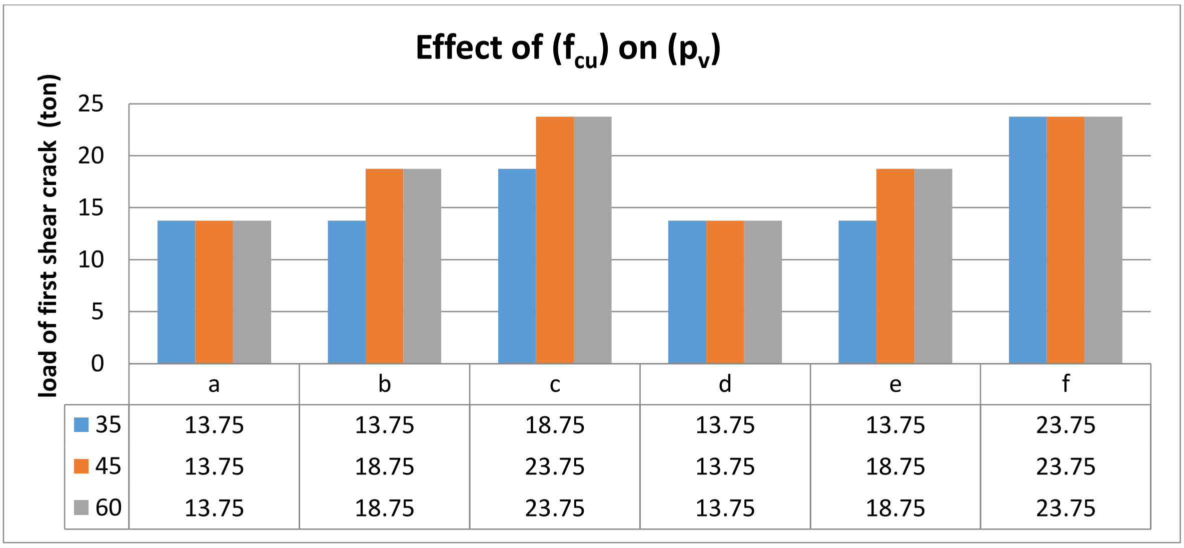

Figure 9: Effect of characteristic strength (f_{cu}) on load of first shear cracks (p_v)

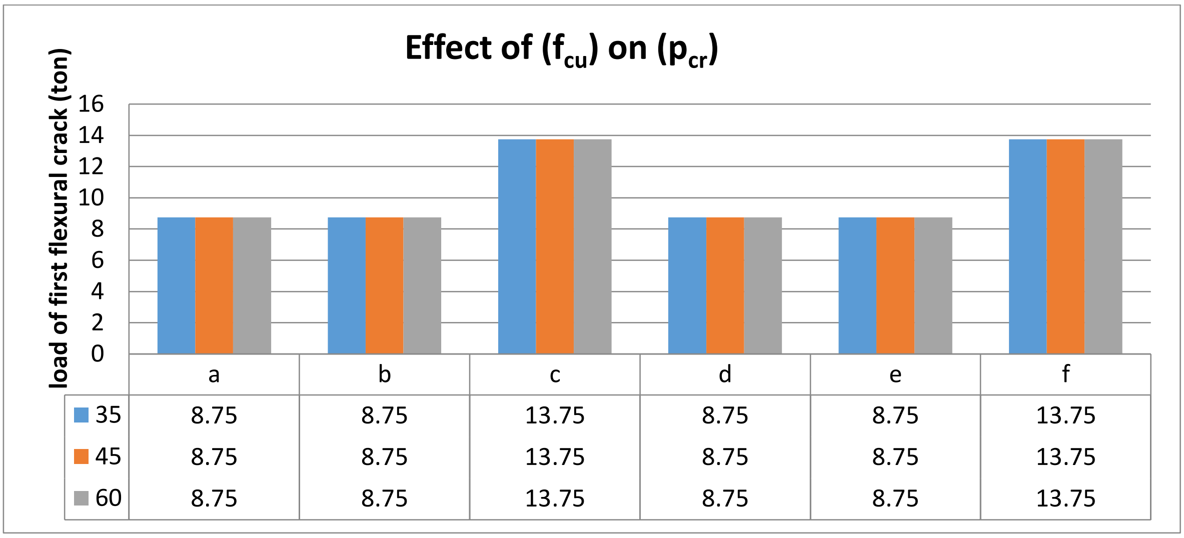

Figure 10: Effect of characteristic strength (f_{cu}) on load of first flexural cracks (p_{cr})

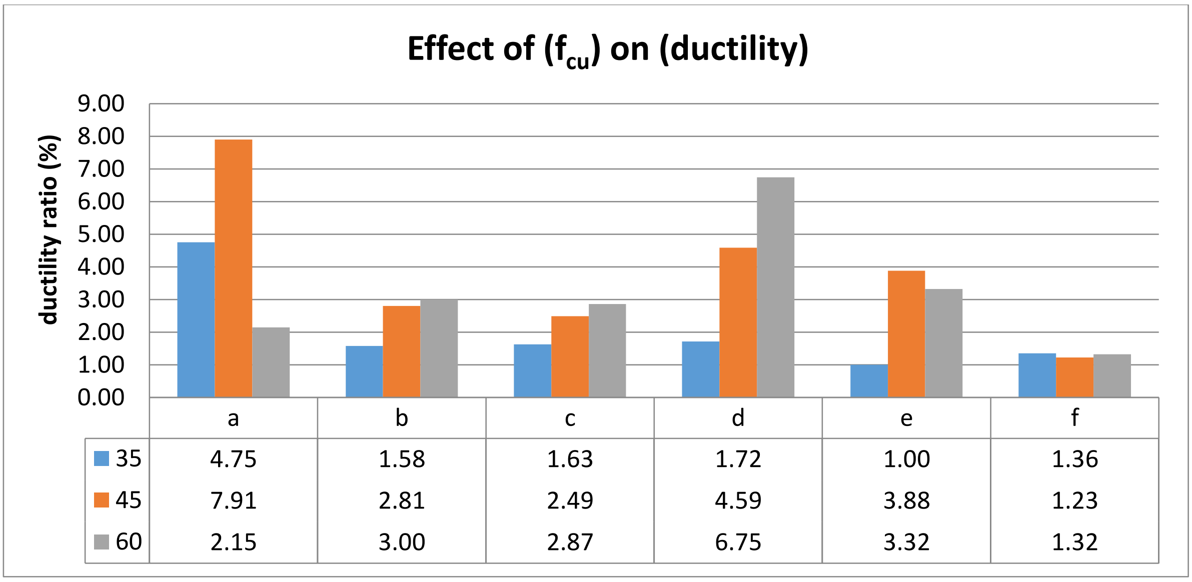

Figure 11: Effect of characteristic strength (f_{cu}) on ductility ratio (%).

Effect of stiffness ratio between column and wall (tc/tw) on ultimate horizontal load capacity, load of first shear cracks, load of first flexural cracks, and ductility can be demonstrated by Figures 12, 13, 14, and 15 respectively. Samples are assembled through a table beneath every single bar-chart according to Table (7).

Table (7) Samples assembly for the case of effect (t_c/t_w)

	a	b	c	d	e	f	g	h	j
group (1)	1	2	3	7	8	9	13	14	15
group (2)	4	5	6	10	11	12	16	17	18

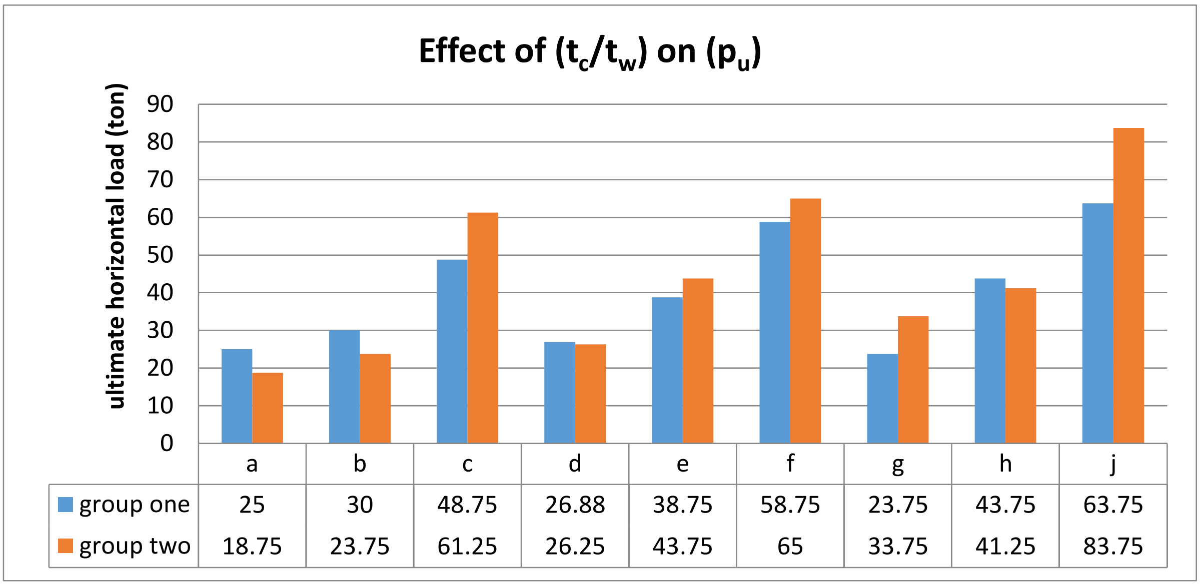

Figure 12: Effect of stiffness ratio (t_c/t_w) on ultimate horizontal load (p_u)

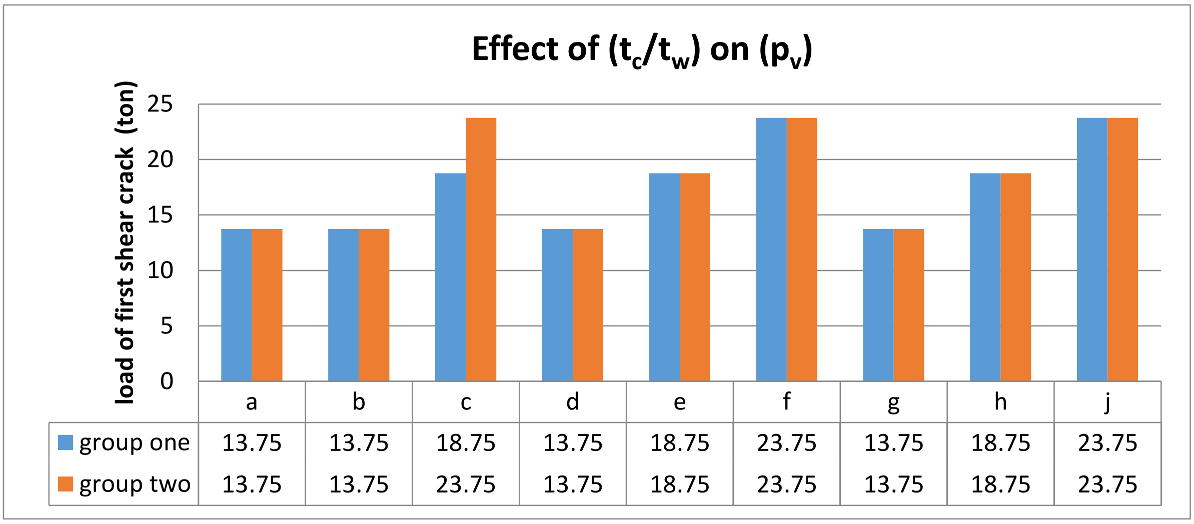

Figure 13: Effect of stiffness ratio (t_c/t_w) on load of first shear cracks (p_v)

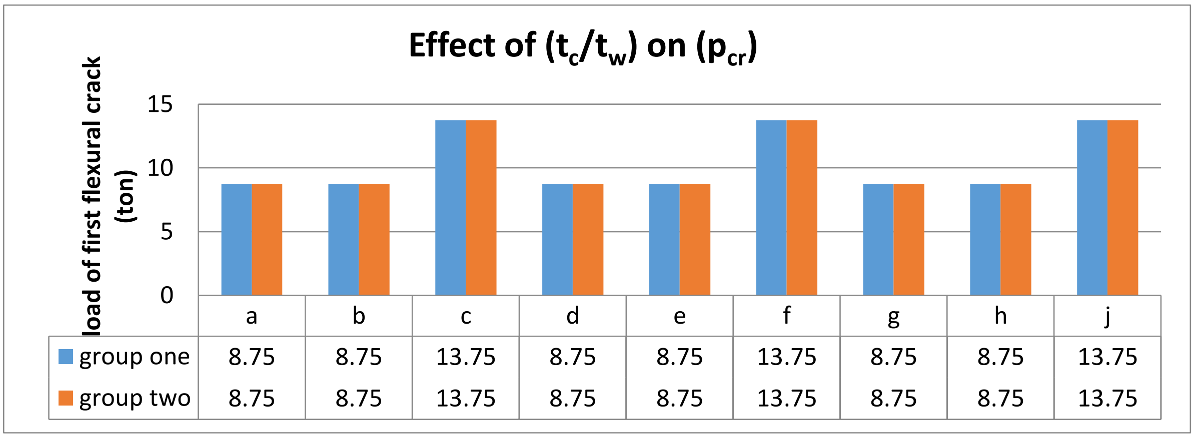

Figure 14: Effect of stiffness ratio (t_c/t_w) on load of first flexural cracks (p_{cr})

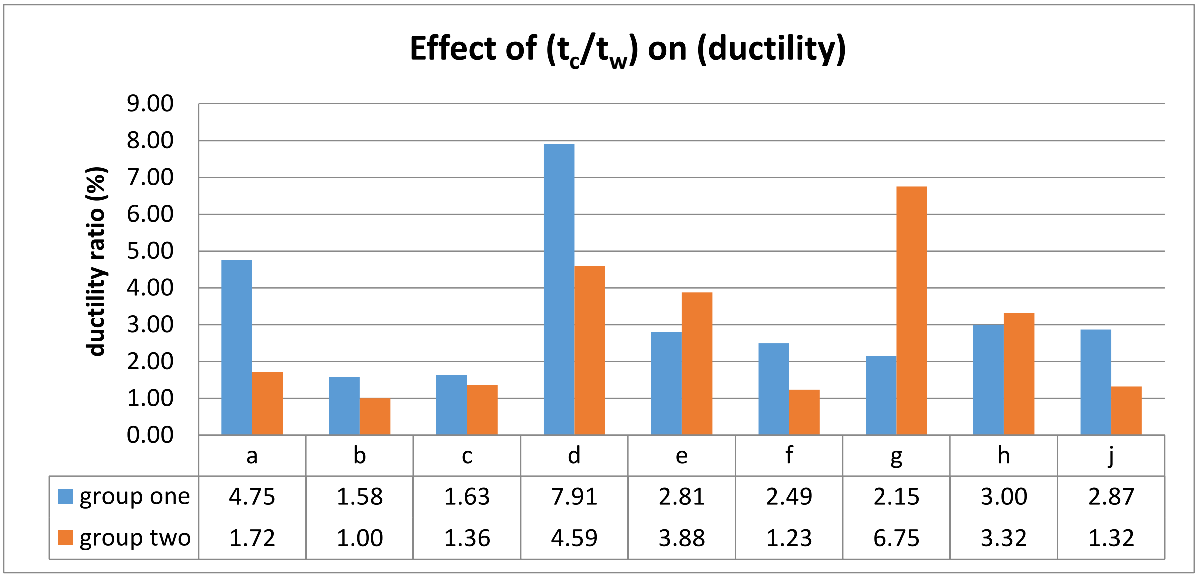

Figure 15: Effect of stiffness ratio (t_c/t_w) on ductility ratio (%).

5. Conclusions

According to the results obtained from the present non-linear analysis of coupled shear walls supported on two columns, the following conclusions may be drawn:

1- Ultimate horizontal load capacity is direct proportion with characteristic strength (f_{cu}). Increasing the characteristic strength (f_{cu}) from 35 to 45 MPa, and from 45 to 60 MPa, would lead to an increase in ultimate horizontal load capacity by nearly 25%, 11.68%, respectively. However, the ultimate horizontal load capacity would climb by about 10.61%, if the stiffness ratio went up from 37.5% to 51.25%.

2- First shear cracks are occurred mainly in transfer beam as well as connecting beams. If the characteristic strength (f_{cu}) climbed from 35 to 45 MPa, load of first shear cracks would go up by about 32.43%, whereas, increasing the characteristic strength (f_{cu}) from 45 to 60 MPa would not affect significantly on the position of first shear cracks. On the other hand, the position of first shear cracks does not be affected enormously by the variation in the stiffness ratio between column and wall.

3- Increasing or decreasing the characteristic strength (f_{cu}) and the stiffness ratio (tc/tw) would not affect significantly on the position of first flexural cracks. The position of these cracks mainly occurred in transfer beam. Load of first flexural cracks is direct proportion with characteristic strength (f_{cu}) and the stiffness ratio (tc/tw) but with a slight rate of increase.

4- Ductility of the whole system is direct proportion with characteristic strength (f_{cu}). Rising the characteristic strength (f_{cu}) from 35 to 45 MPa, and from 45 to 60 MPa, would lead to an increase in ductility by nearly 91%, 15%, respectively. Conversely, Ductility of the whole system would decrease to 13.89%, if the stiffness ratio (tc/tw) climbed from 37.5% to 51.25%.

6. References

[1] ANSYS user's manuals, "Structural Analysis Guide", Release 12.0, ANSYS Inc. Southpointe 275 Technology Drive Canonsburg, PA 15317, April 2009.

[2] Egyptian Code of Practice, ECP-203, "Design and Construction of Reinforced Concrete Structure", Ministry of Building Construction, 2007.

[3] ACI Committee 318, "Building Code Requirements for Reinforced Concrete", American Concrete Institute, Farmington Hill, Michigan, 2008.

[4] Morgan, A.S., "Linear and Nonlinear Analysis of Coupled Shear Walls Supported on Columns", M. Sc., Thesis, Structural Engineering Department, Faculty of Engineering, Cairo University, 222 pp, 1992.

[5] Khaled, A.A., "Nonlinearity of Coupled R.C. Systems Part I: Coupled Shear Walls Supported on Columns", M. Sc., Thesis, Structure Engineering Department, Faculty of Engineering, Tanta University,2004.

[6] H. J. Pam, A. K. H. Kwan and M. S. Islam, "Proceedings of the Institution of Civil Engineers", "Structures and Buildings 146", November 2001, Issue 4, Pages 381-389.

[7] Martinez, S., NiIson, AH. , And Slate, F.O., "Spirally-Reinforced High-Strength Concrete Columns", Research Report No. 82-10, Department of Structural Engineering, Cornell University, Ithaca, Aug. 1982.

[8] K.J. Willam, and E. P. Warnke, "Constitutive Model for Tri-axial Behavior of Concrete", Seminar on Concrete Structures Subjected to Tri-axial Stresses, International Association of Bridge and Structural Engineering Conference, Bergamo, Italy, 1974.

[9] ACI code, MacGregor, "Reinforced Concrete Mechanics and Design", Sixth Edition, 2011.

[10] Tavarez, F.A.,"Simulation of Behavior of Composite Grid Reinforced Concrete Beams Using Explicit Finite Element Methods", Master's Thesis, University of Wisconsin-Madison, Madison, Wisconsin, 2001.

[11] Coull, A., "Simplified Elasto-Plastic Analysis of Coupled Shear Walls", Proc. Instu. Civ., Part 2, 1982, 73, June, 365-381.

[12] Salonikios, T. N., "Analytical Prediction of the Inelastic Response of RC Walls with Low Aspect Ratio", Journal of Structural Engineering, Vol. 133, No. 6, June 2007, pp. 844-854.